388 KSME International Journal, Vol. 12, No. 3, pp. 388~395, 1998

Molecular Dynamics Simulation for Microfracture Behavior of Material

Young-suk Kim* and Jun-young Park**

(*Received June 5, 1997*)

Recently, quasimolecular dynamics has been successfully used to simulate the deformation characteristics of solid materials in actual size material. In quasimolecular dynamics, which is an attempt to bridge the gap between atomistic and continuum simulations, molecules are aggregated into large units, called quasimolecules, to evaluate the large scale material behavior.

In this paper, a 2-dimensional numerical approach using quasimolecular dynamics has been performed to simulate the crack initiation and propagation behavior of a Cu-plate subjected to uniform bending. The bending simulation of the Cu-plate has clarified the effects of aspect ratio and the existence of surface imperfection upon the fracture behavior of the specimen.

Key Words: Bending Deformation, Crack Propagation, Molecular Dynamics

1. Introduction

An investigation on fracture behaviors related with micro-crack growth of industrial materials is of interest, for example, to engineers, mathematicians, and geologists. Recently, many numerical sutdies at the microscopic level have been successfully performed in order to investigate the micro-crack growth and fracture behaviour of solid materials at the atomistic or molecular level using molecular dynamics (MD) (Decelis *et al.*, 1983). Decelis *et al.* (1983) analysed the crack tip process with molecular dynamic simulation. Recently a number of numerical analyses for microscale material behaviors subjected to various deforming processes such as tension (Izumi and Katake (1993), Inoue *et al.* (1995)) and cutting process (Isono and Tanaka, 1996) were performed. Kitagawa *et al.* (1993) analysed the atomic change of structure around the crack-tip under Mode II. These studies were made possible because of recent advances in computer performance. Nevertheless, material size that can be analysed is limited because the material of actual size is composed of a huge number of molecules.

Recently Greenspan's quasimolecular dynamics (QMD) (1986) approaches make it possible, in that molecules are aggregated into a large units, called virtual quasimolecules (Greenspan (1986, 1989)). Using QMD approaches, Greenspan (1986, 1989), Ashurst and Hoover (1976), and Choi and Ryu (1996) simulated the crack and fracture development of a copper plate subjected to tensile loading. However, few investigations of QMD to the industrial applications Greenspan (1986, 1989), Choi and Ryu (1996), Kim and Park (1996)) have been performed except Kim and Park's work (1996) for bending fracture problem. The bending type fracture of a solid material frequently occurs in structures such as power plants due to excessive unsymmetric loading conditions. The analytical and experimental characterization of the bending fractures is, therefore, of considerable interest.

In this paper, the fracture behavior of a Cu-plate subjected to uniform bending is investigated numerically within the framework of Greenspan's QMD method. Moreover, the effects of aspect ratio of the specimen and the existence of surface imperfection upon fracture behaviors are clarified.

* Department of Mechanical Engineering, Kyungpook National University

** Graduate school, Department of Mechanical Engineering, Kyungpook National University

2. Basic analysis

Let us consider a rectangular Cu-plate which is about 8×19.9186cm. The 6-12 Lennard-Jones potential function for two copper atoms r Å apart is given by (Greenspan (1989))

$$\Phi(r)=-\frac{1.398068\times10^{-10}}{r^6}+\frac{1.55104\times10^{-8}}{r^{12}}(erg). \quad (1)$$

From Eq. (1), the force F interacting between two atoms is derived as follows

$$F(r)=-\frac{8.38840\times10^{-2}}{r^7}+\frac{1.866125\times10}{r^{13}}(dyn). \quad (2)$$

The minimum of $\Phi(r)$ results when $F(r)=0$, at $r=2.46$ Å. We assume that the Cu-plate is composed of quasimolecules, the faced-centered cubic structure, and also the distance between the two neighbors is 0.2cm on the plane (1 1 1). If the distance between two adjacent quasimolecules is assumed infinitesimally smaller than 0.2cm, we can get more accurate results like as the molecular dynamics. But the simulation for this case takes more time than the case of 0.2cm. In this sense, the distance, 0.2cm, has no special meaning. Then, the resulting arrangement is shown in Fig. 1.

The number N* of atoms in the plate is,

$$N^*=\frac{8\times10^8}{2.46}\cdot\frac{19.9186\times10^8}{2.46\times\sin 60^\circ}=30.41123707\times10^{16} \quad (3)$$

A quasimolecular mass m from the total mass is given by

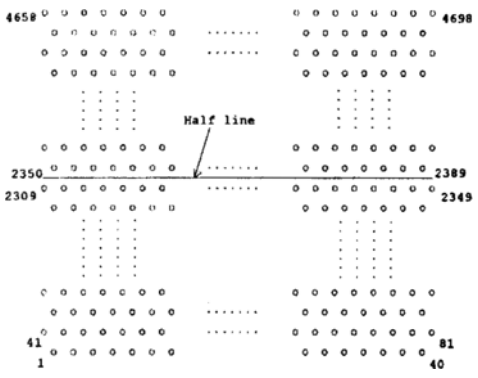

Fig. 1 The initial arrangement for the thick specimen of Cu-plate under bending

$$m=N^*\times1.0542\times10^{-22}/4698=6.824079\times10^{-9}(g) \quad (4)$$

in which we assumed that the total mass is distributed over the 4698 quasimolecules.

The total energy E^* of the system of atoms is

$$E^*=3\times(30.41123707\times10^{16})\times(-3.15045\times10^{-13})$$
$$=-2.8742725\times10^5(erg) \quad (5)$$

Now assume that the force F between two quasimolecules is given by

$$F(R)=\frac{G}{R^3}+\frac{H}{R^5} \quad (6)$$

in which R is measured in centimeters. From the condition that $F(0.2)=0$ and total energy E equals E^*, Eq. (6) takes the specific form

$$F(R)=-\frac{3.262974315}{R^3}+\frac{0.130518972}{R^5} \quad (7)$$

The force acting between two molecules which are separated by a distance of 4. 92 Å, i. e. twice the mean distance 2. 46 Å between two molecules, is negligible due to its very small value compared to weight. We can also apply this property to quasimolecules.

Now, we introduce a normalizing constant α such that at a distance 0.4cm the force between quasimolecules is small relative to their weight. If we define "small relative to weight" to mean 0.1% of the effect of weight, then we must have

$$\alpha\left|-\frac{3.262974315}{(0.4)^3}-\frac{0.130518972}{(0.4)^5}\right|<(0.001)\cdot(980)\,m \quad (8)$$

which results in our choice $\alpha=1.25\times10^{-10}$ (Greenspan, 1986) where the number 980 is the acceleration of gravity. The dynamical equation for the motion of each quasimolecule is

$$m\frac{d^2\boldsymbol{R}_i}{dt^2}=(1.25\times10^{-10})\sum\left[\left(-\frac{3.262974315}{(R_{ij})^3}+\frac{0.130518972}{(R_{ij})^5}\right)\frac{\boldsymbol{R}_{ji}}{|\boldsymbol{R}_{ij}|}\right] \quad (9)$$

in which $\boldsymbol{R}_i$ is a position vector of the point P_i, and $\boldsymbol{R}_{ij}$ is a position vector with initial point P_i and terminal point P_j. The summation is taken over the neighbors of P_i. From Eq. (5) and introducing the computationally convenient transformations $R^*=4R$, $T^2=10t^2$, Eq. (9) reduces to

$$\frac{d^2\boldsymbol{R}_i^*}{dT^2} = \Sigma\left[\left(-\frac{1.530099184}{(R_{ij}^*)^3}+\frac{0.979263473}{(R_{ij}^*)^5}\right)\frac{\boldsymbol{R}_{ij}^*}{R_{ij}^*}\right] \tag{10}$$

Now, for solving Eq. (10) numerically, we adopt the leap-frog method, a type of Verlet method which is frequently used in MD simulation. For a positive time Δt, let $t_k = k\Delta t$, where $k = 0, 1, 2, \cdots\cdots$. Here, we assume that the number of particles is N. Also, at t_k let P_i of mass m_i be located at $r_{i,k}$, with velocity $v_{i,k}$, and acceleration $a_{i,k}$. Then the leap-frog formulas, which relate position, velocity and acceleration, are expressed as follows:

$$\begin{aligned} \vec{v}_{i,1/2} &= \vec{v}_{i,0} + \frac{(\Delta t)}{2}\cdot \vec{F}_{i,0}/m_i \\ \vec{v}_{i,k+1/2} &= \vec{v}_{i,k-1/2} + (\Delta t)\,\vec{F}_{i,k}/m_i, \quad k = 1, 2, \cdots \\ \vec{r}_{i,k+1} &= \vec{r}_{i,k} + (\Delta t)\,\vec{v}_{i,k+1/2}, \quad k = 0, 1, 2, \cdots \end{aligned} \tag{11}$$

In order to simulate crack initiation and propagation behavior in QMD it is necessary to break the quasimolecular bond when the force acting between two neighboring quasimolecules reaches a certain limit. In this study we introduce the separating criterion of quasimolecular bond recommended by Ashurst and Hoover(1976), there the quasimolecular bond is broken when the distance between two neighborhood quasimolecules reaches the distance R* at which dF/dR* first becomes negative. From Eq. (10), then, R* = 1.06667 (Fig. 2).

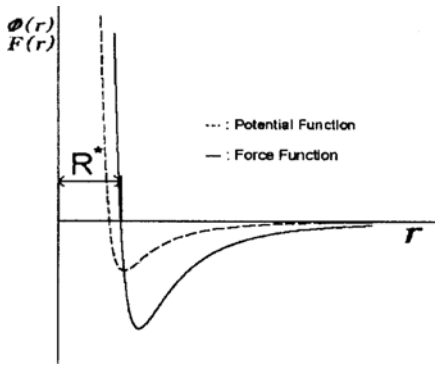

Fig. 2 Potential and force function

3. Numerical simulation models

Figure 1 shows the initial arrangement of quasimolecules for a relatively thick specimen (the Model I case). In order to generate naturally the crack initiation and propagation under tensile strain, a geometrical imperfection of the specimen is introduced as a V-notch shape on the upper convex surface of the specimen as shown in Fig. 3. The size of the specimen of the Cu-plate is a 8cm × 19.9186cm which gives an aspect ratio of 1 : 2.5.

To compute the position change and the force for every quasimolecule, a constant-displacement boundary condition at both ends was applied. During pure bending simulation, the arc length of the neutral axis of the specimen is kept at a constant value and the quasimolecules of both ends are assigned to turn by unit degree per unit time as shown in Fig. 4.

The boundary conditions for bending simulation are given by

$$\begin{bmatrix} X' \\ Y' \end{bmatrix} = Q\begin{bmatrix} X \\ Y \end{bmatrix} - D$$

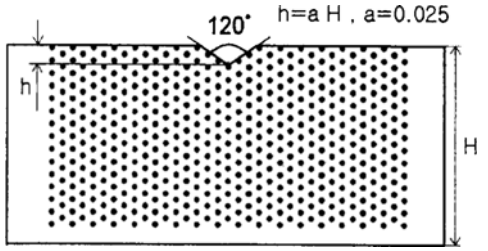

Fig. 3 The initial imperfection of the specimen on the upper convex surface

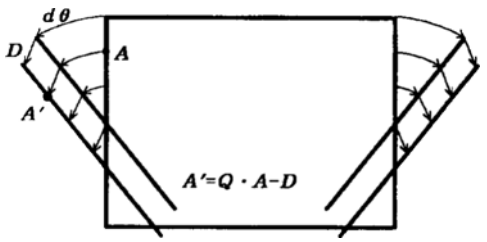

Fig. 4 Displacement boundary condition of quasimolecules at both ends

$$= \begin{bmatrix} \sin \Delta\theta & \cos \Delta\theta \\ \cos \Delta\theta & -\sin \Delta\theta \end{bmatrix} \begin{Bmatrix} X \\ Y \end{Bmatrix} - \begin{Bmatrix} l - \frac{1}{\Delta\theta} \cdot \sin \Delta\theta \\ \frac{1}{\Delta\theta} - \frac{l}{\Delta\theta} \cdot \cos \Delta\theta \end{Bmatrix} \quad (12)$$

where l is the half length of the neutral line. The Q matrix represents the rotation transformation of the coordinate axis, and the D matrix is introduced to take into consideration that the neutral line of the specimen has a curvature in proportion to the turning angle.

The turning angle θ is measured from the vertical line to the quasimolecules on the end line. A time step ΔT is taken as 0.1 and degree step $\Delta\theta$ is kept at 0.01. Therefore, $d\theta/dT = 0.1$ (deg/time).

4. Numerical Results and Discussion

Figure 5 shows the initial state and arrangement of the quasimolecules of the thick specimen with a V-notch on the upper surface (Model Case 1). The deformation behaviors and crack propagation tendency during bending are shown in Figs. 6~10. Their figures correspond to turning angles of $\theta = 17°$, 18°, 19°, 21° and 22°, respectively.

Until the specimen bends to $\theta = 17°$ (Fig. 6), the specimen seems to deform uniformly with pure bending, in which generally the upper convex surface is under tensile stress and the lower concave surface under compressive stress. However, when the turning angle reaches $\theta = 18°$ (Fig. 7), a visible crack generated from the notch occurs due to the high tensile stress acting on the upper convex surface, at which the bond of quasimolecules are first broken. The crack generated from the notch propagates deeply into the specimen as the specimen continues to bend.

Figure 8 for the deformed state of $\theta = 19°$ illustrates that the crack propagation extends deeply into the center of the specimen. As can be seen in the figure, we can see a more realistic crack propagation pattern in that firsty the front of the crack may propagate into two directions, an almost vertical direction to the neutral axis and is an inclined direction to the vertical direction. This crack propagation into two directions ceases as the bending of the specimen proceeds, and the crack propagation along a major direction becomes predominant as the bending proceeds. This pattern of crack propagation is repeated during bending. Therefore the rough fractured

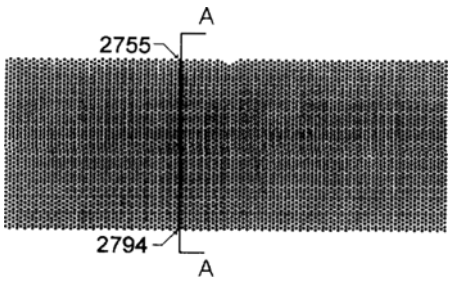

Fig. 5 The initial state of thick specimen with notch before bending

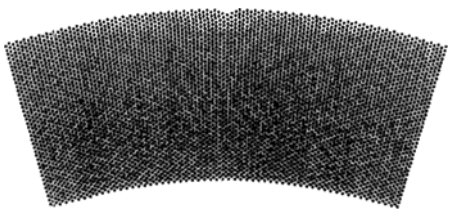

Fig. 6 Deformed state of thick specimen with notch at $\theta = 17°$ with an aspect ratio of 1:2.5

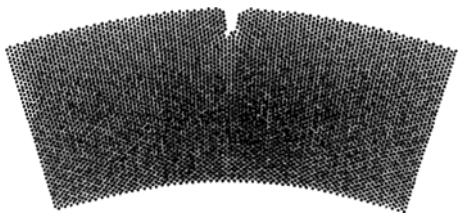

Fig. 7 Deformed state of thick specimen with notch at $\theta = 18°$

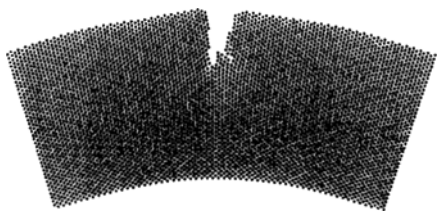

Fig. 8 Deformed state of thick specimen with notch at $\theta = 19°$

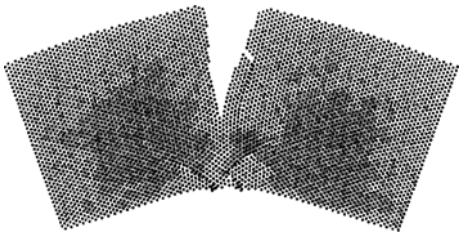

Fig. 9 Deformed state of thick specimen with notch at $\theta=21°$

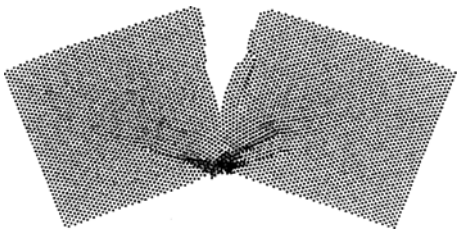

Fig. 10 Deformed state of thick specimen with notch at $\theta=22°$

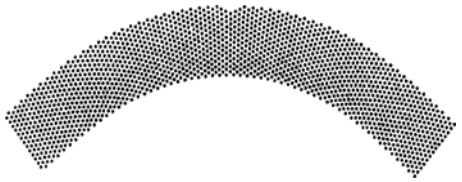

Fig. 11 Deformed state of thin specimen with notch at $\theta=40°$ with an aspect ratio of 0.32:2.5

Fig. 12 Deformed state of thin specimen with notch at $\theta=45°$

surface will appear. This crack propagation tendency is similar with the actual fracture phenomena of ductile materials subjected to bending stress.

Figure 9 shows the deformed state at $\theta=21°$. In this case, the crack proceeds almost up to the neutral axis of the specimen in the major direction. Also there we can observe the rough fractured surface due to the stepped propagation pattern as discussed above. Moreover at the lower concave surface of the specimen some dense quasimolecules area subjected to high compressive stress seem to appear. This dense area of quasimolecules at the concave side of the specimen may contribute to the development of plastic hinges (compression instability).

Figure 10 shows the deformed state at $\theta=22°$, at which a plastic hinge on the concave side is fully developed. High energy will be accumulated at the plastic hinge area as expected from Eq. (1) because the density of molecules is high there.

Next, in order to clarify the effect of the thickness upon the fracture behavior of the specimen, simulation for a relative thin specimen of aspect ratio 0.32:2.5 (called Model II case) was performed under the same boundary condition as case I.

Figures 11~12 show the deformed states at $\theta=40°$ and $\theta=45°$ respectively. In Fig. 11 the comparatively thin plate bents uniformly until $\theta=40°$ without any crack propagation around the notch area and any dense quasimolecules area at concave side. This deformation characteristic of uniform bending of thin plate is proven everywhere by actual phenomena. From the comparison between the deformed state of the thin material in Fig. 11 and that of the thick material, it is certain that in spite of the existence of the same magnitude of imperfection, the thin material deforms more uniformly than the thick material. This could be explained as follows. In pure bending, the magnitude of tensile stress acting on the upper fiber of the specimen is almost proportional to the thickness of the specimen, and therefore the tensile stress acting on the upper surface for the thin specimen is lower than that for the thick specimen. A similar analogy can be introduced in the case of the concave side. This makes the thin material deform more uniformly without any fracture occurring at the convex side and any dense quasimolecules at the concave side.

The fully developed V-shape fracture is observed in Fig. 12 for the deformed state at $\theta=45°$. Compared to Fig. 10 of the thick specimen, it is certain that the fracture of the specimen develops

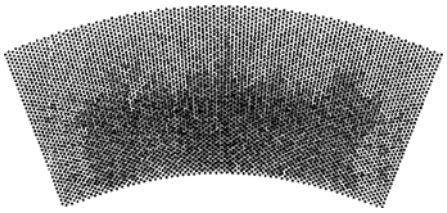

Fig. 13 Deformed state of thick specimen without notch at $\theta=22°$ with an aspect ratio of 1:2.5

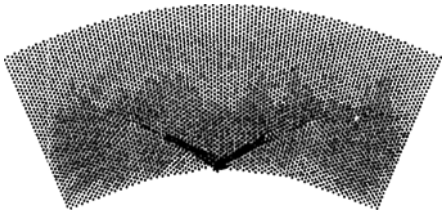

Fig. 14 Deformed state of thick specimen without notch at $\theta=24°$

at the front of the V-notch only in a direction perpendicular to the neutral axis. Moreover the fractured surface for the thin specimen is more fine and has a regular V-shape.

Figures 13~14 illustrate the deformed states at $\theta=22°$ and 24° in the case of no surface imperfection for the thick specimen. This case (Model III case) was chosen to investigate the effect of the existence of the surface imperfection upon fracture behaviors of the specimen.

Figure 13 shows no signs of fracture occurring on both sides of the specimen until the specimen bends to $\theta=22°$. However, in Fig. 14 for the case of $\theta=24°$, some dense quasimolecular area in shear band-like form is developed at the concave side. As the specimen continues to bend this phenomenon becomes more noticeable. Therefore, it can be concluded that the specimen with no notch is apt to produce the compression instability at the concave side but not tensile fracture at the convex side during bending.

Figures. 15~18 illustrate the longitudinal force distributions interacting between two neighborhood quasimolecules along the y-axis positions of the quasimolecules with respect to the turning angle in Model I case. In these figures the X-coordinate represents a magnitude of longitudinal

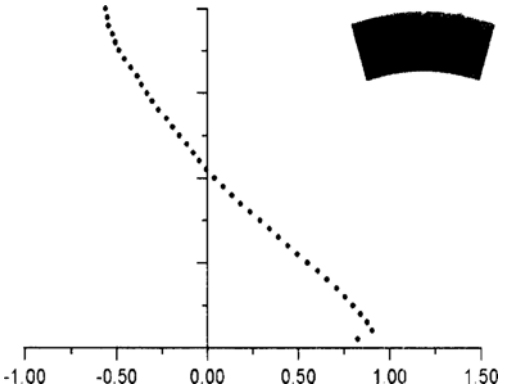

Fig. 15 The force distribution along y axis position of $\theta=17°$

force and Y-coordinate represents the y-axis position of quasimolecules. The measurement of the interacting forces was performed at the vicinity of the notch area because of stress propagation velocity. Here, the forces at the quasimolecules located between the 2755th and the 2794th molecules along the A-A section are measured as shown in Fig. 5.

In the case of Fig. 15 for a bending angle of $\theta=17°$, the longitudinal forces of each quasimolecule are distributed almost uniformly with proportion to the y-distance of each quasimolecule from the neutral axis, center line of the specimen. This assures that the uniform bending deformation is preserve at $\theta=17°$ as discussed in the deformed state of Fig. 6.

However, when the crack on the convex side propagates deeply into the center of the specimen as shown in Figs. 7~10 according to an increase of the bending angle, the longitudinal forces which were acting on the fracture occurring area are released rapidly. Therefore, the magnitude of the force acting on the fractured area finally approaches zero as can be seen in Fig. 16, Fig. 17 and Fig. 18 corresponding to $\theta=18°$, $\theta=19°$, and $\theta=21°$, respectively.

In Fig. 16 for a bending angle of $\theta=18°$, the proportional force distribution like Fig. 15 is first broken, and the force acting on the upper convex surface diminishes. Next, the area where the force approaches zero becomes wider in Fig. 17 for the case $\theta=19°$. The state shown in Fig. 18 for $\theta=21°$

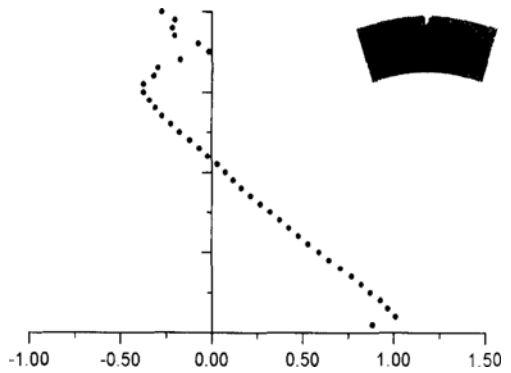

Fig. 16 The force distribution along y axis position of $\theta=18°$

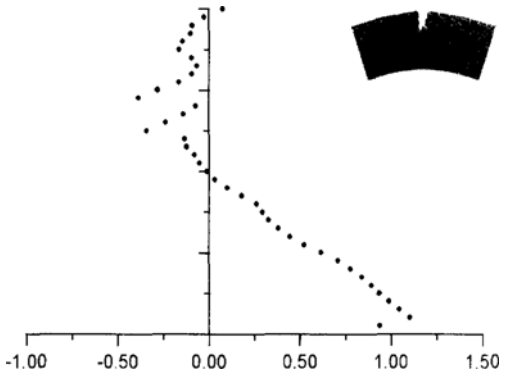

Fig. 17 The force distribution along y axis position of $\theta=19°$

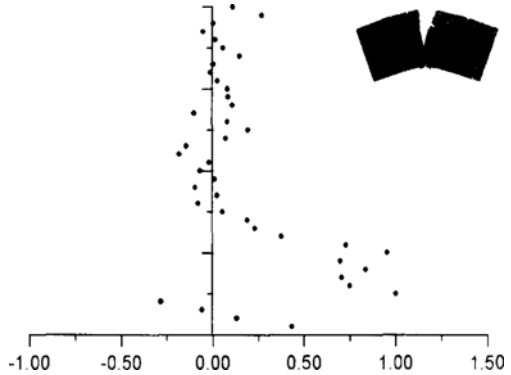

Fig. 18 The force distribution along y axis position of $\theta=21°$

depicts the force acting on the fractured area at the convex side, where it becomes almost zero; therefore, the fractured area transmits no more force during bending. Moreover, we found compressive unstable states on the concave side which implies the possibility of the occurrence of a plastic hinge as discussed in Fig. 9.

5. Conclusions

According to the results of a quasimolecular simulation for bending, we clarified the fracture behavior and crack propagation pattern of the specimen. The investigations on the effect of specimen size make clear that the thick plate reaches material fracture more early than thin plates under the same magnitude of surface imperfection. Moreover, comparison between the notch specimen and no notch specimen reveals that the specimen with no notch continues to deform without any fracture on the convex side until $\theta=$ 24°. However, on the concave side a dense quasimolecular area like a shear band localization is observed. From this study we can conclude that the bending operation is very sensitive to imperfections on the outer surface and as the thickness of the specimen thickens the tendency becomes more significant.

Acknowledgement

Financial support from the Korea Science & Engineering Foundation under Grant # 971-1004-022-1 is gratefully acknowledged.

References

Decelis, B., Argon, A. S., and Yip S., 1983, "Molecular Dynamics Simulation of Crack Tip Processes in Alpha-iron And Copper," *J. Appl. Phys.*, Vol. 54, pp. 4864~4878.

Izumi, S., and Katake, S., 1993, "Molecular Dynamic Study of Solid Deformation," *Trans. JSME.* Vol. A59. pp. 263~267.

Inoue, H., Akahoshi, Y., Harada, S., and Chobara, H., 1995, "Molecular Dynamics Simulation of Temperature-Dependent Tensile Fracture of Nanoscale Polycrystal," *Trans. JSME.*, Vol. A61., pp. 1813~1818.

Isono, Y., and Tanaka, T., 1996, "Three-Dimensional Molecular Dynamics Simulation of Atomic -Scale Cutting Process Using Pin Tool," *Trans.*

JSME., Vol. A62. pp. 2364~2371.

Kitagawa, H., Nakatani, A., and Shibutani, Y., 1993, "Study on Computational Modelling for Materials with Crystalline Structure," *Trans. JSME.*, Vol. A59., pp. 1834~1841.

Greenspan, D., 1986, "Quasi-Molecular Particle Modeling of Crack Generation and Fracture," *Computers and Structures.*, Vol. 22, pp. 1055~1061.

Greenspan, D., 1989, "Supercomputer Simulation of Cracks and Fractures by Quasimolecular Dynamics," *J. Phys. Chem. Solids.*, Vol. 50, pp. 1245~1249.

Ashurst, W. T. and Hoover, W. G., 1976, "Microscopic Fracture Studies in the Two-Dimensional Trianglar Lattice," *Physcal Review.* B14, pp. 1465~1473.

Choi, D and Ryu, H., 1996, "A computer Simulation of Fractures of Metallic Solids," *Proc. KSME Spring Conf. in Korea,* pp. 102~106.

Kim, Y. and Park, J., 1996, "Analysis of Metallic Solid Fracture by Quasimolecular Dynamic," *Proc. the 47th JSTP Joint Conf.* pp. 457~458.